Stratospheric Nitrous Oxide Altitude Profiles at Various Latitudes

A. L. SCHMELTEKOPF, D. L. ALBRITTON, P. J. CRUTZEN,[1] P. D. GOLDAN, W. J. HARROP, W. R. HENDERSON, J. R. MCAFEE, M. MCFARLAND, H. I. SCHIFF[2] AND T. L. THOMPSON

Aeronomy Laboratory, NOAA Environmental Research Laboratories, Boulder, Colo. 80302

D. J. HOFMANN AND N. T. KJOME

Department of Physics and Astronomy, University of Wyoming, Laramie 82071

(Manuscript received 3 November 1976, in revised form 3 February 1977)

ABSTRACT

A number of N_2O profiles obtained in the troposphere and stratosphere at five latitudes are reported. The variability in the reported stratospheric N_2O mixing ratios is substantial and indicates a strong dependence on both stratospheric transport and photochemistry. A profile obtained at Panama indicates a relatively large transport of N_2O into the stratosphere at low latitudes. This profile represents the first one obtained in the tropics. From the observed data, area-averaged, global vertical eddy diffusion coefficients were derived that were found to be a factor of 1.5 to 3 times larger than those derived by Hunten from data obtained at locations not including the tropics. The derived eddy diffusion profile is heavily weighted by one single profile in the tropics and more observations are needed to substantiate this finding.

The estimated flux of N_2O into the stratosphere was equal to 15×10^{12} g(N) per year and the total stratospheric production of NO_x was estimated to be 1.6×10^{12} g(N) per year. The atmospheric turnover time of N_2O would be 100 years if photochemical reactions were the only sink for atmospheric N_2O.

1. Introduction

Measurements of vertical profiles of N_2O concentrations are essential to our understanding of the earth's ozone layer in several ways. The ozone loss rate in the stratosphere below 45 km is primarily controlled by the catalytic action of oxides of nitrogen (NO_x) whose principal source is the reaction of N_2O with $O(^1D)$ (Crutzen, 1970, 1971). The source of N_2O, in turn, is microbiological activity in soils and waters. The possibility of future increases in the N_2O flux into the stratosphere due to increased usage of industrial nitrogen fertilizers has recently received considerable attention (Crutzen, 1972, 1974). Understanding this transport of N_2O is of vital importance when considering the natural variations or anthropogenic perturbations in the ozone layer.

Predictions of such effects have made use to date mainly of so-called one-dimensional empirical models. Such models incorporate chemistry in a rather detailed manner. On the other hand, the description of the many ways in which transport of chemical species can take place is highly parameterized. The effects of all possible types and scales of transport is described by introducing an effective eddy diffusion that is defined as a function of altitude. The numerical values of the coefficient are determined empirically by fitting the theoretical vertical distributions of one or more trace constituents to the observed profiles.

Both CH_4 and N_2O are suitable choices for the derivation of eddy diffusion coefficients since these tracers have no sources above ground level. Furthermore, both compounds are sufficiently stable to be mixed evenly in the troposphere while being destroyed in the stratosphere by processes that are reasonably well understood. However, since CH_4 is lost in the stratosphere by reactions with $O(^1D)$ and especially with HO, whose altitude concentration profile is somewhat indefinite, an uncertainty is introduced by the use of CH_4 as a tracer. The principal loss process for N_2O through photolysis can be estimated with greater certainty.

Nevertheless, only CH_4 has previously been measured in sufficient detail to make possible a derivation of an eddy diffusion coefficient profile for use in models. The profile due to Ehhalt *et al.* (1974) is an average of measurements of whole air samples obtained from nine balloon flights at Palestine, Tex., and two rocket flights from White Sands, N. M. These sites have the advan-

[1] Also at the National Center for Atmospheric Research, Boulder, Colo. (NCAR is sponsored by the National Science Foundation).

[2] Permanent affiliation: York University, Downsview, Ontario, Canada.

TABLE 1. Data pertaining to the flights.

Flight	Location		Date	Number of Samples	Tropopause altitude (km)
1	Wyoming	41°N, 105°W	June 1975	3	16.0
2	Saskatchewan	51°N, 102°W	August 1975	5	11.5
3	Colorado	40°N, 105°W	September 1975	4	—
4	Wyoming	41°N, 105°W	December 1975	2	—
5	Antarctic	78°S, 167°E	January 1976	10	8.5
6	New Mexico	32°N, 106°W	February 1976	2	—
7	Panama	9°N, 79°W	April 1976	5	17.1
8	Wyoming	41°N, 105°W	May 1976	3	12.0
9	Alaska	63°N, 147°W	May 1976	5	9.5
10	Alaska	63°N, 147°W	May 1976	4	8.9
11	Wyoming	41°N, 105°W	July 1976	5	15.0
12	Wyoming	41°N, 105°W	July 1976	4	13.6
13	Wyoming	41°N, 105°W	August 1976	5	14.0

tage of being located at a latitude (32°N) that roughly bisects the Northern Hemisphere but the disadvantage of being in a region with downward mean motions in the lower stratosphere. It is not clear, therefore, how representative these data are of global average conditions. A question also exists as to whether values for eddy diffusion coefficients derived from one tracer are consistent with values obtained from another.

In view of these considerations, mixing-ratio altitude-profile measurements for N_2O have been obtained at a number of locations and those results are reported here. In addition, the data provide a first opportunity to derive a globally averaged eddy diffusion coefficient and to estimate the global production of NO_x from N_2O oxidation in the stratosphere.

2. Sample acquisition and analysis techniques

Stratospheric whole air samples at ambient pressure are acquired by means of a balloon-borne sampling package containing five evacuated 7.5 l stainless steel sampling spheres with automated opening and closing mechanisms for each sphere. The five spheres are clustered about an electronic control package which cuts the package free from its balloon, opens and closes each sphere at preselected altitudes and telemeters operational data, temperatures and pressures to ground monitoring stations. The construction, sample sphere preparation, operation, deployment and recovery of this package have been described in detail elsewhere (Schmeltekopf *et al.*, 1976). Only a few of the pertinent details will be mentioned here.

The sampling package is borne aloft by two small rubber or one plastic balloon. The relative simplicity of the system has enabled us to make launchings at a number of sites resulting in some desirable latitude and seasonal coverage. The operational data concerning these flights are given in Table 1. When the balloon bursts at stratospheric altitudes of the order of 35 km, it is cut away and the package descends on a parachute. Shortly thereafter the sampling spheres are preprogrammed to open, fill to ambient pressure and reseal, each at a different altitude during descent. This procedure yields five samples between the maximum altitude and a point just below the anticipated tropopause altitude. After impact and recovery the spheres are returned to the laboratory for analysis by gas chromatography.

The steel spheres are electropolished, assembled by inert gas welding, and tested to insure leak rates below 3×10^{-10} atm cm^3 s^{-1}. Since the recovered samples are analyzed for other components in addition to N_2O, subsequent to flight 7 of Table 1 the spheres were passivated with hexamethyldisilazane to occupy inner surface sites activated by the welding process. Although never a problem for the analysis of N_2O, such active sites can otherwise demonstrably remove a significant fraction, if not all, of some other trace constituents originally present at the ppb level. The spheres are then evacuated to pressure less than 10^{-7} torr, while being heated to 200°C before being sealed off for flight.

The gas samples are obtained while the package is descending on its parachute in order to avoid contamination known to be present in the wake of the balloon. Each sample sphere is fitted with an inlet tube that extends below the package and crash frame. These inlet tubes are evacuated with their respective sample spheres and thus contain no stagnant air carried aloft with the package. The opening mechanism physically removes a small vacuum-tight can that covers the end of the inlet tube. Thus we are assured not only of the cleanliness of the sample sphere but also that the gas returned to the laboratory for analysis is indeed representative of the atmosphere where the container was opened.

The heights at which sampling occurs are calculated from the pressure, temperature, and opening and closing telemetry data. One of the largest uncertainties in the height arises because the package is falling on its parachute during the filling time. Both the descent rate and the filling time are functions of altitude. At 30 km, the

package falls at approximately 30 m s^{-1} and the filling time is 20 s. At lower altitudes the descent rate is slower and the filling time somewhat shorter. Since most of the filling occurs during the first few seconds after opening, the effective sampling altitude can be determined to better than ±150 m at 30 km and to better than ±50 m below 25 km.

The acquired gas sample analysis is performed in the laboratory by means of gas chromatography using an electron capture detector. It has been known for some time (Wentworth *et al.*, 1971, 1973) that N_2O has a measurable electron capture cross section which increases significantly with increasing temperature. Advantage is taken of this fact by operating a Ni^{63} detector at 350°C, which is the maximum temperature attainable with the equipment available. At this temperature, the electron capture cross section of N_2O is about a factor of 10^3 lower than that for $CFCl_3$, for which electron capture detection techniques are widely used, but since the ambient tropospheric concentration of N_2O is about 300 ppbv, compared to 0.150 ppbv for $CFCl_3$, the sensitivity is quite adequate. As a result, this technique, which was simultaneously developed by several laboratories in addition to this one, is being rapidly disseminated and is currently in use both in the United States and in western Europe for the routine measurement of N_2O in atmospheric samples.

The analysis is performed on a 3.2 mm stainless steel tubular column approximately 4.3 m long packed with 100–150 Mesh Porasil "C". A typical chromatogram is shown in Fig. 1, which shows the resolution of N_2O, CF_2Cl_2 and $CFCl_3$ from the O_2 in the air sample. The sample size for the chromatogram shown was 60 torr in a 19 cm^3 sample loop. Subambient pressure samples are accommodated by the use of an evacuated sample inlet system and a pressure measuring sensor. The vacuum line is carefully trapped to avoid sample loop contamination from backstreaming pump vapors.

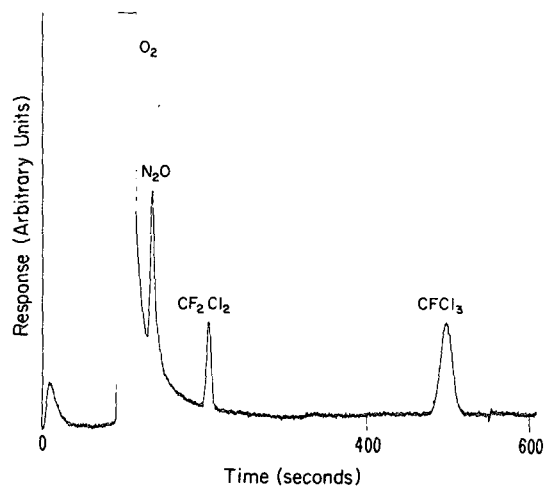

FIG. 1. Typical chromatogram showing the resolution of N_2O, CF_2Cl_2 and $CFCl_3$ from the O_2 in an air sample.

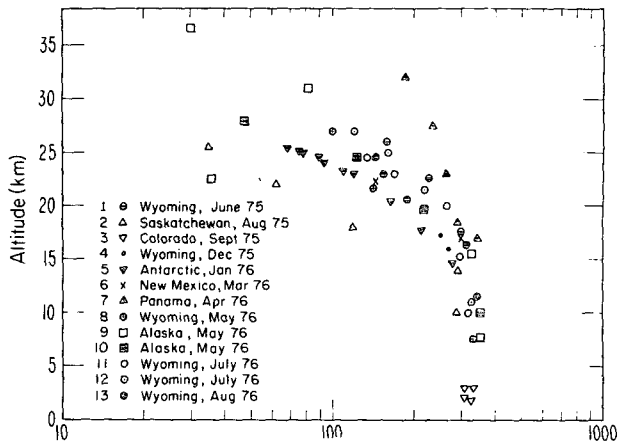

FIG. 2. Measured N_2O mixing ratios (ppbv) for the flights in Table 1.

The absolute number of molecules of N_2O (or of CF_2Cl_2, $CFCl_3$, or any other detected species) is proportional to the peak height or peak area. Quantitative measurement is made by means of calibration with gas samples prepared on a dynamic dilution system. The use of this system either eliminates or allows the evaluation of storage stability problems associated with very dilute gases, a problem that is of paramount importance in the quantification of trace constituent measurements at or below the ppb level. The reproducibility of this calibration technique is demonstrated by the excellent agreement of the N_2O mixing ratio measured at or below the tropopause on numerous balloon flights, as discussed in the next section.

3. Experimental results

The results of the measurements for the flights in Table 1 are shown in Fig. 2, in which the N_2O mixing ratios are plotted as a function of altitude. Generally, the data show good agreement in the troposphere and a great deal of variation in the stratosphere.

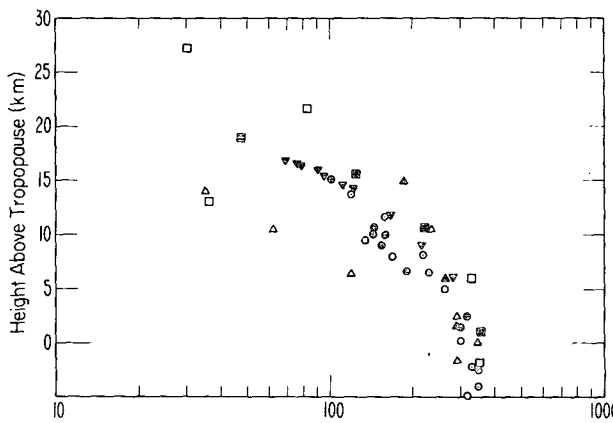

FIG. 3. Measured N_2O mixing ratios (ppbv) as a function of height above the tropopause.

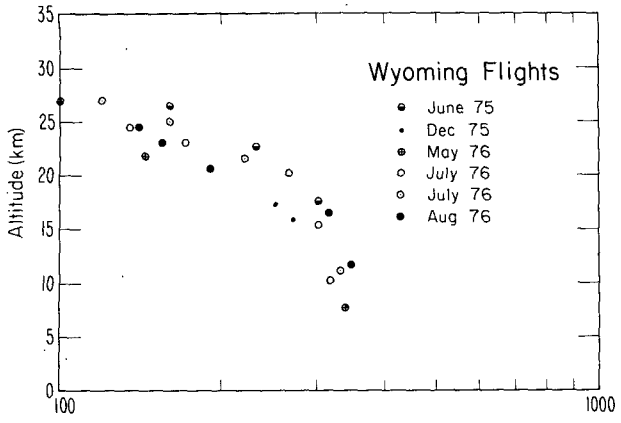

FIG. 4. Measured N_2O mixing ratios (ppbv) for the Wyoming flights.

The consistency of the data in the troposphere shows up more clearly in Fig. 3, which is identical to Fig. 2 except that height above the tropopause is used and flight 4 is omitted for lack of tropopause data. The tropopause (see Table 1) is defined here, somewhat subjectively, as the altitude at which the temperature profile changes from a large negative gradient to a much smaller or near-zero gradient. It may be noticed that, despite some substantial variability in tropospheric N_2O mixing ratios (320±40 ppbv), there does not seem to exist any characteristic altitude variation in the troposphere, contrary to stratospheric conditions.

One would expect a much larger variability in the N_2O mixing ratio in the stratosphere because of the strong dependence of the photolysis rate on latitude and season, especially as a function of altitude. The influence of transport processes by the stratospheric wind systems remains, however, very important. The short-term variation can be seen directly in the data. This is better illustrated in Fig. 4, which isolates the data from the Wyoming flights already shown in Fig. 2. In particular, the time variability is substantial over the four week period including the two July and the August flights in 1976. The two Alaskan flights, 11 days apart, show an even larger variation (see Fig. 5). In fact, the presence of the maximum in the first Alaskan flight would necessitate a source of N_2O in that region if only vertical transport were effective. In contrast to these, the data for the Antarctic show far less variability for the particular period of the measurements. The 10 data points are actually from two flights of five samples each and two days apart.

Much of the stratospheric variability can only be explained by variations in the stratospheric wind systems. In the first Alaskan flight the only reasonable explanation would involve the presence of a wind in the 20–25 km altitude range bringing in an air volume from a region with different characteristics, namely a far smaller N_2O content. This sort of profile also points out the possible danger of comparing a one-dimensional theoretical model profile with a single measured profile. Although the transport effect is obvious here, since N_2O has such a simple photochemical behavior, it would be disguised for species with a more complicated one and could be quite misleading. The full extent of the variability contributed by the dynamics cannot be seen, however, until the profiles are actually used to calculate effective eddy diffusion coefficients.

4. Derivation of eddy diffusion coefficients

In a one-dimensional empirical model, the time rate of change of a constituent [X] is governed by the continuity equation

$$\frac{d}{dt}[\mathrm{X}]=-\frac{d}{dz}\Phi_z-L+P, \tag{1}$$

where L and P are the photochemical destruction and production rates, respectively. The net upward flux Φ_z is represented by

$$\Phi_z=-K_z[\mathrm{M}]\frac{d}{dz}\frac{[\mathrm{X}]}{[\mathrm{M}]}, \tag{2}$$

where [M] is the concentration of air molecules. The effect of transport is contained in the flux divergence term through the effective eddy diffusion coefficient K_z.

Since N_2O has been produced naturally at a fairly constant rate, it is not unreasonable to assume on the average that steady-state conditions prevail in the stratosphere, and $d[\mathrm{X}]/dt=0$. Additionally, N_2O is not produced in the stratosphere, so that $P=0$. Then (1) and (2) give

$$\frac{d}{dz}K_z[\mathrm{M}]\frac{d}{dz}\frac{[\mathrm{N_2O}]}{[\mathrm{M}]}=L. \tag{3}$$

Given that one can measure or estimate the other quantities, K_z can be obtained from solutions of (3) for each measured N_2O altitude profile. Integration be-

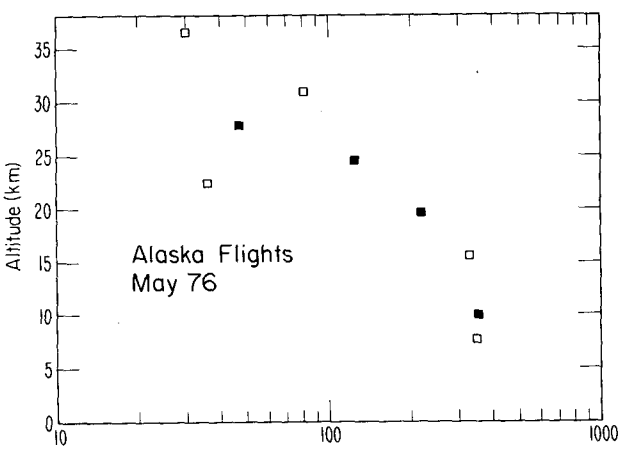

FIG. 5. Measured N_2O mixing ratios (ppbv) for the Alaska flights.

tween a particular altitude z and infinity gives for $K_z(z)$ at that height:

$$K_z(z)=\frac{-1}{[\mathrm{M}](z)\dfrac{d}{dz}\dfrac{[\mathrm{N_2O}]}{[\mathrm{M}](z)}}\int_z^\infty L(z)dz,$$

$$=\frac{-\Phi(z)}{[\mathrm{M}](z)\dfrac{d}{dz}\dfrac{[\mathrm{N_2O}]}{[\mathrm{M}](z)}}. \quad (4)$$

The quantities in the denominator of (4) are the background air molecule concentration [M] which is well known, and the mixing ratio of N_2O, which is our measured quantity. The major loss process for N_2O is photolysis, i.e.,

$$N_2O+h\nu(\lambda<230\text{ nm})\rightarrow N_2+O(^1D). \quad (5)$$

In this study the N_2O photolysis rates were calculated as a function of altitude, latitude and season. The main uncertainties relate to the solar radiation output in the photodissociation spectral region ($\lambda<230$ nm). The solar irradiances adopted for this study (Simon, 1974) are larger than those recently reported by Heroux and Swirbalus (1975) by about a factor of 2 between 180 and 194 nm. An additional uncertainty arises from the penetration of the solar radiation through the highly structured absorption spectrum of oxygen below about 200 nm. This uncertainty may be estimated from the study of Kockarts (1971) to be a factor of 2 in this spectral region. Approximately 30% of the N_2O photodissociation occurs at wavelengths <200 nm. The overall uncertainty in the photodissociation rate is estimated to be no greater than $\pm 50\%$.

Additional loss of N_2O occurs through reactions with $O(^1D)$:

$$O(^1D)+N_2O\rightarrow 2NO, \quad (6a)$$

$$O(^1D)+N_2O\rightarrow N_2+O_2. \quad (6b)$$

The $O(^1D)$ is produced from the uv photolysis of O_3. The rate constant for the overall reaction [(6a)+(6b)] has recently been measured over the stratospheric temperature range of interest (Davidson *et al.*, 1976). The $O(^1D)$ height profiles are taken from the two-dimensional time-dependent model of Crutzen (1975), but since reaction (6) contributes at most 20% to the total N_2O loss rate, discrepancies between actual and calculated $O(^1D)$ densities should not lead to serious errors.

The integral in (4) may then be evaluated numerically in the region where measurements are taken. Unfortunately, a large fraction of the loss occurs in the region above our highest measurements, and the contributions to the flux from this region above must be estimated.

The method used to estimate this contribution was to extrapolate the measured mixing-ratio profiles upward. Curve fitting in the region at the top of the measured range was used in the first few (2–4) kilometers above the top measurement point. A simple exponential behavior was assumed at higher altitudes. Some corroboration for this procedure was obtained by comparison with model N_2O altitude profiles using K_z values based upon the CH_4 measurements (Crutzen, 1975). The profiles used to calculate individual K_z profiles are shown in Fig. 6.

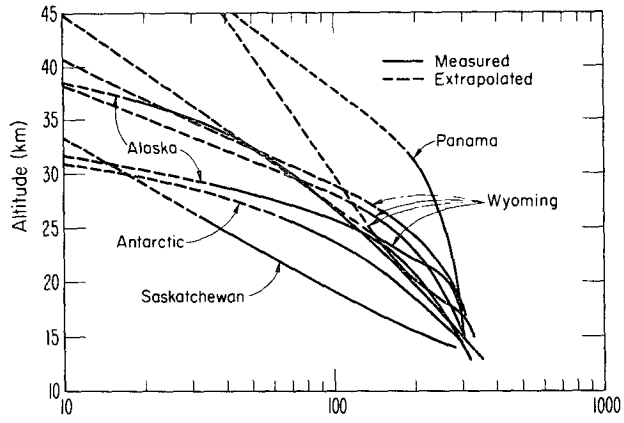

FIG. 6. N_2O mixing ratio (ppbv) profiles used to calculate eddy diffusion coefficients.

The errors in the flux at the top of the measurement range due to the above (somewhat arbitrary) extrapolation procedures are not severe. Since the maximum loss rate occurs at or just above the top of the measurement range, the major contribution to the integral in (4) occurs within the measurement range or at worst, just slightly above it where the extrapolation errors are smallest. Conversely, the flux contribution is small at higher altitudes where the extrapolation errors could be largest. To indicate the sensitivity to extrapolation procedure, we also extrapolated to a N_2O density at 45 km as much as a factor of 10 smaller than previously used by assuming a pure exponential behavior between

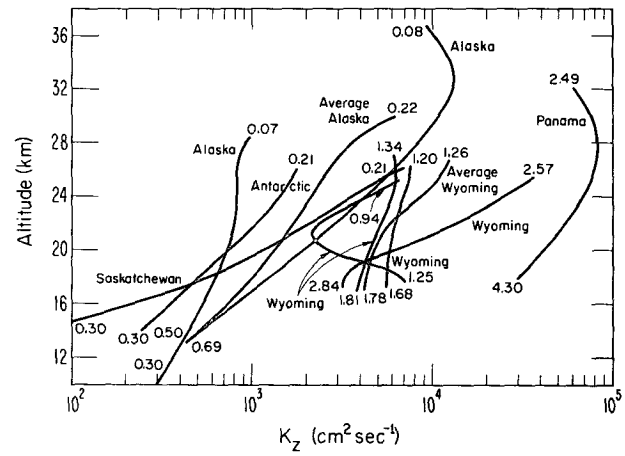

FIG. 7. Individual eddy diffusion coefficient profiles.

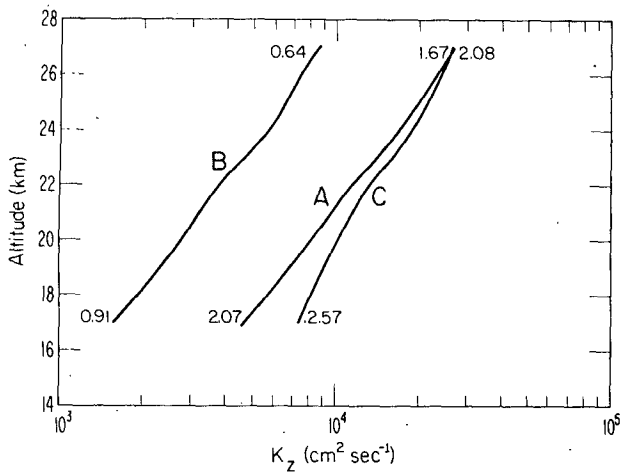

FIG. 8. Average $\bar{K}_z$ profiles: A, all data; B, all data less Panama; C, all data less Saskatchewan.

this value and the highest measured point (32 km) for the Panama flight. The result was only a 50% reduction in the calculated flux at 32 km. Similar changes for other flights produced even smaller reductions.

Integration of (4) for each of the N_2O profiles produced the K_z profiles presented in Fig. 7. The numbers shown above and below each curve represent the derived fluxes Φ_z at the top and bottom of the altitude range over which measurements were taken; the difference between the two values is the integrated loss in this range. The additional profiles that are shown correspond to averaging the two Alaskan flights and the four Wyoming flights.

The large differences in the K_z profiles demonstrate that the location for any measurement is an important consideration. Most likely, the differences in derived K_z values are the result of the neglect of other forms of transport rather than a representation of real variations in eddy vertical mixing as a function of latitude. In the case of the Panama measurements, vertical upwelling, consistent with current concepts of mean meridional circulation at that latitude, could supply the large upward flux. Conversely, mean downward stratospheric motion would be required to explain the results from the Saskatchewan measurements. Since accurate estimates of such flows are not available, it is difficult to estimate their contribution to the vertical fluxes. Horizontal fluxes and horizontal diffusion could also be a contributing factor. In addition, the steady-state assumption may be questionable since the eddy-diffusion time constants $\tau \approx H^2/K_z$, where H is the scale height, become large compared to those for the photochemical loss processes when K_z is small. For these reasons, the individual K_z profiles probably have little physical reality.

Of greater interest to stratospheric modellers for inclusion in one-dimensional models are mean, globally averaged, $\bar{K}_z$ profiles. If (2) is integrated over a spherical surface.

$$\bar{K}_z \int_0^{\pi} \int_0^{2\pi} [\mathrm{M}] \frac{d}{dz} \frac{[\mathrm{N_2O}]}{[\mathrm{M}]} \sin\theta d\theta d\phi = -\int_0^{\pi} \int_0^{2\pi} \Phi_z \sin\theta d\theta d\phi, \quad (7)$$

where the integrals represent the net upward flux. Since profiles have only been obtained at five locations (Panama, Wyoming-averaged, Saskatchewan, Alaska-averaged and Antarctic), the integrals must be approximated by sums that are weighted by the approximate area factor $\cos\nu_i$, where ν_i is the local latitude for the ith profile. Thus

$$\bar{K}_z \sum_{i=1}^{5} [\mathrm{M}]_i \frac{d}{dz} \frac{[\mathrm{N_2O}]_i}{[\mathrm{M}]_i} \cos\nu_i = -\sum_{i=1}^{5} \phi_{zi} \cos\nu_i. \quad (8)$$

The average $\bar{K}_z$ can then be defined as

$$\bar{K}_z = \frac{\sum_{i=1}^{5} \Phi_{zi} \cos\nu_i}{\sum_{i=1}^{5} [\mathrm{M}]_i \frac{d}{dz} \frac{[\mathrm{N_2O}]_i}{[\mathrm{M}]_i} \cos\nu_i}. \quad (9)$$

The results are shown in Fig. 8, where curve A shows the average $\bar{K}_z$ altitude profile obtained from (9) using all the measurements, and curve B represents the profile which would have been derived if the Panama data had not been available for the analysis. The influence of the Panama data is obvious, and our $\bar{K}_z$ profile could be in error if the single Panama flight was not representative. Curve C was obtained by omitting the Saskatchewan data, which had the largest decrease with altitude and seemed somewhat inconsistent with the other mid-latitude to high-latitude data. Fortunately, the effect is not large. The derived N_2O flux for curve A is about 2×10^9 molecules cm^{-2} s^{-1}, corresponding to a world-wide annual production of 15 000 kton (N) in the absence of any other sinks.

Curve A of Fig. 8 is also compared in Fig. 9 to some of the vertical eddy diffusion coefficients used by other modelers. There is general agreement with those models that show an increase with altitude in the lower stratosphere. There is yet no unique procedure for deriving representative global $\bar{K}_z$ values because of limited amounts of observations and uncertainties in photochemistry. The spread in the $\bar{K}_z$ values between different models at a given altitude can be as high as a factor of 10. The average value obtained from our N_2O data lies predominantly within this spread. Johnston *et al.* (1976) have recently analyzed the data on the dissipation of excess C^{14} from the stratosphere during the 1963–70 period on the basis of various $\bar{K}_z$ profiles

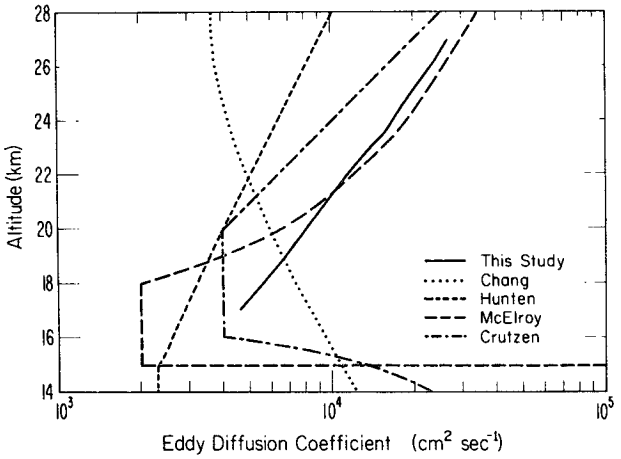

FIG. 9. Comparison of $\bar{K}_z$ profiles. The modelers are Chang (1974), Hunten (1975), McElroy *et al.* (1974) and Crutzen (private communication).

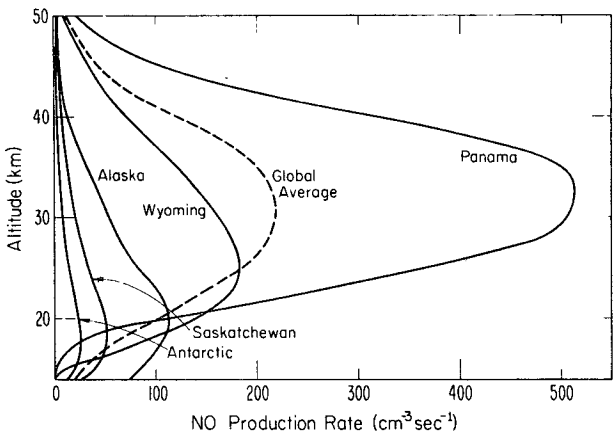

FIG. 10. NO production rates for measured and extrapolated N_2O profiles.

and found the best agreement with that of Hunten (1975). Our average profile has a shape similar to that of Hunten, but the absolute values are a factor of 1.5 to 3 times larger. If the contribution from the tropics had not been available, the resulting $\bar{K}_z$ profile (curve B in Fig. 8) would have been quite close to Hunten's above 23 km.

5. Production rate of NO_x

The oxides of nitrogen in the stratosphere are believed to be formed mainly from the reaction of N_2O with $O(^1D)$ atoms to produce nitric oxide, as in reaction (6a). The N_2O height profiles in Fig. 6 can therefore be used to calculate local NO production rates. Although the rate constant for the overall reaction [(6a)+(6b)] has been measured as a function of temperature, the branching ratio between the two channels has been determined only at room temperature. Since there is very little temperature dependence on the overall rate constant, it is very likely that the room temperature branching ratio of 1:1 will also apply at stratospheric temperatures. Since (6a) produces two NO molecules per $O(^1D)$ atom, the NO production rate equals the contribution to the N_2O loss rate due to the total reaction with $O(^1D)$. The resulting NO production rates are shown in Fig. 10.

The significance of the individual curves should not be overemphasized, since the N_2O and $O(^1D)$ profiles are not exactly representative of seasonal averages. Nevertheless, it is interesting to note the extreme variation in NO_x production rates from large values at low latitudes to small values at high latitudes. In fact, the data suggest that about 75% of the stratospheric NO_x production from N_2O occurs equatorward of 30° latitude. It is also interesting to note the change in the altitude of maximum production with latitude and the fact that this maximum occurs within our measuremetn range in all cases.

If the individual NO_x production profiles in Fig. 10 are weighted by the cosν area factor and averaged, the result is the curve labeled "global average." By integrating this curve the average column stratospheric NO_x production is found to be 4.5×10^8 mol cm^{-2} s^{-1}.

6. Summary

Measurements of N_2O at a number of locations spanning the latitude range from 63°N to 78°S show that mixing ratios are relatively constant (to within ±15%) in the troposphere and the lowest part of the stratosphere. However, considerable spatial and temporal variability is observed in the stratospheric distribution. These variations suggest the importance of transport. Because of this variability, occasional disagreements between one-dimensional model profiles and individual measurement profiles may be expected. Hopefully, the theoretical profiles represent average conditions that can only be obtained by averaging a sufficient number of observations.

Nevertheless, the globally averaged values of $\bar{K}_z$ obtained from the data presented here, by virtue of the fact that they contain a tropical stratospheric profile, probably represent an improvement over the values obtained from the more geographically limited CH_4 data, despite the fact that our vertical range is smaller and the data are restricted to local summer. Future flights, planned to extend the measurements to higher altitudes and to include more low-latitude locations, should further improve the data base. This would permit a better characterization of the variability and a better appreciation of the errors involved in the one-dimensional parameterization of transport processes.

Calculations of expected NO_x production rates using the N_2O profiles show a tremendous variation from

large values at low latitudes to very little at high latitudes. We estimate a global annual production of NO_x of 1600 kton (N) in the stratosphere, most of which is transported into the troposphere. The stratospheric sink of N_2O is estimated to be 15 000 kton (N) per year, so about 10% of the N_2O molecules entering the stratosphere are converted to NO_x molecules. If photochemical reactions in the stratosphere would provide the only sink for N_2O, its atmospheric turnover time would equal 100 years. Simultaneous measurements of O_3 in the future would permit a more accurate assessment of the NO_x production rate, which is vital when considering stratospheric ozone destruction from both natural and human causes.

REFERENCES

Chang, J. S., 1974: Simulations, perturbations, and interpretations. *Proc. Third Conf. Climatic Impact Assessment Program*, U. S. Dept. of Transportation, 330–341. [Available from NTIS as DOT-TSC-OST-74-15.]

Crutzen, P. J., 1970: The influence of nitrogen oxides on the atmospheric ozone content. *Quart. J. Roy. Meteor. Soc.*, **96**, 320–325.

——, 1971: Ozone production rates in an oxygen-hydrogen-nitrogen atmosphere. *J. Geophys. Res.*, **76**, 7311–7327.

——, 1972: SST's—A threat to the earth's ozone shield. *Ambio*, **1**, 41–51.

——, 1974: Estimates of possible variations in total ozone due to natural causes and human activities. *Ambio*, **3**, 201–210.

——, 1975: A two-dimensional photochemical model of the atmosphere below 55 km. Estimates of natural and man-caused ozone perturbations due to NO_x. *Proc. Fourth Conf. Climatic Impact Assessment Program*, U. S. Dept. of Transportation, 264–279. [Available from NTIS as DOT-TSC-OST-75-38.]

Davidson, J. A., H. I. Schiff, G. E. Streit, C. J. Howard and A. L. Schmeltekopf, 1976: Temperature dependence of $O(^1D)$ rate constants for reactions with N_2O, H_2, CH_4, HCl, and NH_3. Submitted to *J. Chem. Phys.*

Ehhalt, D. H., L. E. Heidt, R. H. Lueb and N. Roper, 1974: Vertical profiles of CH_4, H_2, CO, N_2O and CO_2 in the stratosphere. *Proc. Third Conf. Climatic Impact Assessment Program*, U. S. Dept. of Transportation, 153–160. [Available from NTIS as DOT-TSC-OST-74-15.]

Heroux, L., and R. A. Swirbalus, 1976: Full-disk solar fluxes between 1230 and 1940 Å. *J. Geophys. Res.*, **81**, 436–439.

Hunten, D. M., 1975: Estimates of stratospheric pollution by an analytic model. *Proc. Nat. Acad. Sci.*, **72**, 4711–4715.

Johnston, H. S., D. Kattenhorn and G. Whitten, 1976: Use of excess carbon 14 data to calibrate models of stratospheric ozone depletion by supersonic transports. *J. Geophys. Res.*, **81**, 368–380.

Kockarts, G., 1971: Penetration of solar radiation in the Schumann-Runge bands of molecular oxygen. *Mesopheric Models and Related Experiments*, C. Fiocco, Ed., D. Reidel, 160–176.

McElroy, M., S. Wofsy, J. Penner and J. McConnell, 1974: Atmospheric ozone: Possible impact of stratospheric aviation. *J. Atmos. Sci.*, **31**, 287–300.

Schmeltekopf, A. L., P. D. Goldan, W. J. Harrop, T. L. Thompson, D. L. Albritton, M. McFarland, A. E. Sapp and W. R. Henderson, 1976: Balloon-borne stratospheric grab-sampling system. *Rev. Sci. Instrum.*, **47**, 1479–1485.

Simon, P., 1974: Balloon measurements of solar fluxes between 1960 Å and 2300 Å. *Aeron. Acta*, **A123**, 1–14.

Wentworth, W. E., E. Chen and R. Freeman, 1971: Thermal electron attachment to nitrous oxide. *J. Chem. Phys.*, **55**, 2075–2078.

——, and R. Freeman, 1973: Measurement of atmospheric nitrous oxide using electron capture detection in conjunction with gas chromatography. *J. Chromatography*, **79**, 322–324.